Lawrence Berkeley Laboratory

UNIVERSITY OF CALIFORNIA, BERKELEY, CA

Materials & Molecular Research Division

Submitted to the International Journal of Fracture - An Invited Review

FATIGUE IN CERAMICS

A. G. Evans

July 1979

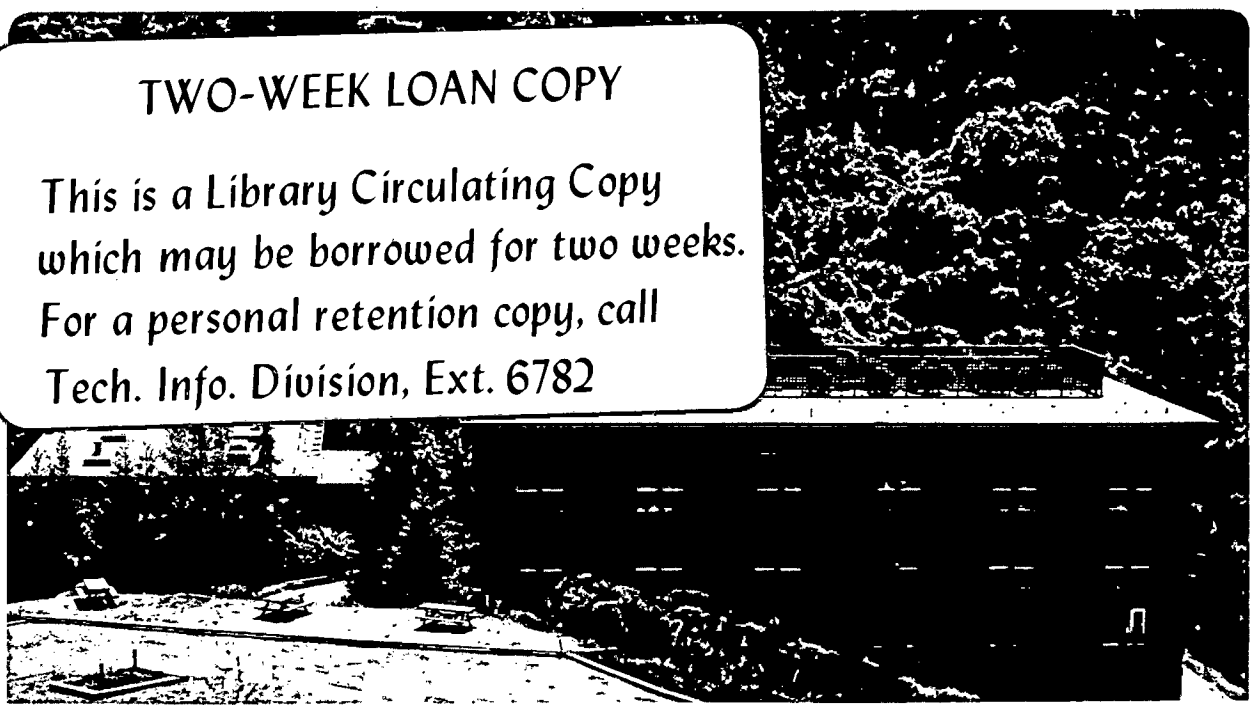

Prepared for the U. S. Department of Energy
under Contract W-7405-ENG-48

DISCLAIMER

FATIGUE IN CERAMICS

A. G. Evans
Dept. Materials Science and Mineral Engineering
University of California
Berkeley, CA 94720

ABSTRACT

The fatigue process in ceramic materials is reviewed. It is shown that there are few cases where fatigue effects have been unequivocally demonstrated. Mechanisms pertinent to the substantiated fatigue conditions are presented and discussed. The needed for further definitive experimentation to deduce the realm of fatigue, and its dependence on mocrostructure, vis-a-vis the fatigue models, is emphasized.

I. INTRODUCTION

The term fatigue has been employed in the ceramics literature to describe a variety of processes that lead to a degradation of mechanical properties with time. For example, static fatigue has been used to describe stress corrosion cracking in glasses and ceramics in the presence of moisture[1,2,3], and the term acoustic fatigue has been introduced to describe the damage accumulation by microcracking that occurs in anisotropic ceramics subject to acoustic waves[4]. This usage represents an important semantic departure from the exclusive use of the fatigue terminology in metals to describe cyclic effects on mechanical property degradation. This review will emphasize cyclic property degradation effects in ceramics, to afford a basis for comparison with the equivalent behavior in metals.

Fatigue has not been extensively studies in ceramics, primarily because the absence of appreciable crack tip plasticity in most ceramics[5] would suggest that fatigue may not be a significant problem in this class of materials. However, the existing fatigue data indicate that fatigue effects may be possible in certain situations. A discussion of their effects will be the primary theme of this review.

Cyclic effects on failure have been reported in situations where, upon detailed analysis, the reported effect has been demonstrated to be a cyclic manifestation of stress corrosion cracking. A discussion of these results will be presented first, to provide a basis for judging the existence of true cyclic effects: wherein cycling leads to crack extension effects that superimpose on the influence of the equivalent steady state stress. Thereafter, the fatigue effects that are judged to exhibit a high

probability of occurence are examined in more detail. In particular, potential fatigue mechanisms will be examined, in order to provide insights into the prerequisites for the onset of fatigue, as well as establishing pertinent fatigue characterization schemes.

Several fatigue strengthening effects have also been reported. Such effects have been noted in glass[6] (referred to as coaxing) and in cements[7]. The strengthening effect occurs if the material is subject to low amplitude cyclic stresses prior to subsequent testing. Similar effects have been observed when materials are subject to small quasi-static stresses[8]. The necessity for cycling in order to achieve the strengthening is thus debatable and no specific attention is devoted to this topic in the present review.

Finally, crack extension is often observed in ceramics during unloading from a compressive condition[9,10]. This behavior can usually be attributed either to residual stresses that develop due to irreversible slippage between the ceramic and the metallic loading platters[9] (c.f., indentation fracture[11]) or to slip induced cracking that is suppressed by the applied compression. These phenomena could be classified as fatigue effects. However, the cyclic damage accumulation that occurs under compressive conditions has not been sufficiently documented to permit this mode of fatigue to be analyzed at this juncture.

2. CYCLIC SLOW CRACK GROWTH

The velocity v of a crack subject to slow crack growth can frequently be characterized by the relation[12];

$$da/dt \equiv v = v_0(K_I/K_c)^n \qquad (1)$$

where a is the crack length, K_I is the stress intensity factor, K_c is the critical stress intensity factor for the material and v_o and n are constrants pertinent to the material and test environment. Noting that the stress intensity factor is related to the stress σ by

$$K_I = \sigma Y \sqrt{a} \tag{2}$$

where Y is a generalized geometric parameter, the crack growth becomes,

$$\frac{da}{a^{n/2}} = \left(\frac{v_o Y^n}{K_c{}^n}\right) \sigma^n(t)dt \tag{3}$$

The variation of the crack growth rate , or of the crack extension, can be deduced for any stress history by insertion of the time dependence of K_I or σ into Eqns. (1) and (3) respectively[13]. For a cyclic stress condition, if fatigue effects are absent, the crack growth should correlate directly with that obtained under quasi-static conditions. For example, the velocity correlation for a sinusoidal stress intensity factor

$$K_I = K_a + K_o \sin\omega t \tag{4}$$

can be obtained by determining the average crack growth rate v_a. From Eqns. (1) and (4), the change in crack length Δa in a time Δt is;

$$\Delta a = \frac{v_o}{K_c{}^n} \int_o^{\Delta t} (K_a + K_o \sin\omega t)^n dt \tag{5}$$

The average velocity is thus,

$$v_a = \frac{\Delta a}{\Delta t} = v_o \left(\frac{K_a}{K_c}\right)^n \frac{1}{\lambda} \int_o^{\lambda} (1 + \zeta \sin\omega t)^n \, dt \tag{6}$$

where $\lambda = 2\pi/\omega$ is the wavelength and $\zeta = K_o/K_a$. Integration gives[13],

$$v_a = v_o \left(\frac{K_a}{K_c}\right)^n \sum_{\ell=0}^{(n/2)} \left[\frac{n!}{(n-2\ell)!\ (\ell!)^2}\right] (\zeta/2)^{2\ell} \tag{7}$$

$$\equiv v_o \left(\frac{K_a}{K_c}\right)^n g$$

Typical values for g are plotted in Fig. 1. Comparison with the quasi-static velocity v_s at the stress intensity factor K_a (Eqn. 1) yields;

$$(v_a/v_s) = g \tag{8}$$

Note that v_a is frequency independent.

Values of g can also be obtained for other cycles[13]. For a saw tooth cycle,

$$g = \sum_{\ell=0}^{n/2} \left[\frac{n!}{(n-2\ell)!\ (2\ell+1)!}\right] \zeta^{2\ell} \tag{9}$$

and for a square wave;

$$g = \sum_{\ell=0}^{n/2} \left[\frac{n!}{(n-2\ell)!(2\ell)!}\right] \zeta^{2\ell} \tag{10}$$

Crack velocity data for glass and for porcelain (Fig. 2) obtained under cyclic and quasi-static conditions[13] correlate well on the basis of Eqn. (7),

suggesting that true fatigue effects are of minor significance in these materials; at least under the conditions used to obtain the test results. Similar conclusions were obtained for glass, by demonstrating the absence of a frequency effect on the average crack velocity[14]. Preliminary data on Si_3N_4 obtained at elevated temperatures (in the creep regime) also indicated an insignificant role of cycling[15]. A crack velocity approach for establishing correlations between cyclic and quasi-static crack growth effects is undoubtedly the preferred approach, since comparisons can be made on the same specimen. However, few such comparisons have been undertaken[13,14,15].

More extensive comparisons have been conducted using time-to-failure experiments. Effective correlation is impeded in the time-to-failure approach by the considerable scatter in results. Progress can only be achieved using a statistical analysis of the data in conjunction with a static (t_s), cyclic (t_c) time-to-failure relation based on the slow crack growth characteristic of the material. The latter can be derived using an analysis comparable to the crack velocity analysis, yielding[13].

$$t_c/t_s = g^{-1} (\sigma_s/\sigma_a)^n \qquad (11)$$

where σ_a is the average cyclic stress and σ_s is the quasi-static stress. Three sets of time-to-failure data are noteworthy. The first, due to Krohn and Hasselman[16], compare static and cyclic failure times at several frequencies under an applied tensile bias. Within the scatter of the data, no significant cyclic fatigue effects can be discerned (Fig. 3). A possible exception is one of the results obtained at the highest frequency (40Hz). However, crack velocity experiments conducted on glass up to very high frequencies (350 Hz) exhibited no fatigue effects[14]. The existence of fatigue

at high frequencies due to non-linear effects near the crack tip cannot, therefore, be substantiated at this juncture. No further consideration is given to this possibility in the present review.

Extensive data have been obtained by Chen and Knapp[17], using a low frequency (0.3 Hz) tension cycle. A careful statistical analysis of the results revealed some unusual trends in the failure time with temperature: and suggested a possible cyclic influence at room temperature, but no effect at 200°C and above (Fig. 4). The significance of these results is difficult to assess. Both the temperature and cyclic stress effects could be dismissed by attributing the apparent trends to batch variability in the various samples selected for testing. However, the possible existence of a fatigue effect must be admitted; a possibility that merits further investigation.

Some recent results obtained by Guiu[18] on alumina suggest that fatigue crack extension may occur in tension/compression cycling (Fig. 5). These results were obtained by comparing the time-to-failure at a steady stress with those obtained for a tension-compression fatigue test (the peak cyclic stress being the same as the steady state stress). The failure time in the fatigue test was consistently smaller than that in the quasi-static test. Considerable care was taken to minimize the formation of extraneous stresses (e.g., stress waves and flexural stresses). Some credence can thus be given to the existence of fatigue in compression/tension cycling, if batch variability effects can be discounted. Crack extension in the compressive half cycle is explored in the following section.

Fatigue tests have been conducted at elevated temperature on Si_3N_4[19]. The results were not obtained over the same range of conditions as quasi-static (creep rupture) tests performed on the same materials and therefore, it is difficult to ascertain whether the data signify a genuine cyclic influence on the failure time. An attempt at extraplation into the same

conditions of temperature and peak stress suggest that cycling does not yield significantly inferior performance, in accord with the crack velocity measurements[15]. However, in principle, the transients that accompany cycling could be important. Additional testing is clearly needed to examine fatigue in the creep regime in order to explore potential creep-fatigue interactions.

A fatigue condition wherein the relation given by Eqn. (7) certainly does not pertain has been unambiguously established in ceramic/metal alloys of the WC/Co type[14]. These materials do not exhibit significant quasi-static slow crack growth, but are highly susceptible to crack growth under cyclic conditions (Fig. 6). The existence of fatigue in this class of materials has been attributed to the metallic phase. This phenomenon is explored in the following section.

3. FATIGUE MECHANISMS

The mechanisms of fatigue that can be proposed for ceramics may depend on the crack structure in the material vis-a-vis the microstructure. In fine grained ceramic polycrystals, fracture criticality is only encountered when the principal crack length substantially exceeds the grain diameter. Potential fatigue mechanisms pertinent to <u>macrocrack</u> growth are thus of greatest interest in these materials. Alternately fracture in coarse grained materials frequently involves the formation and coalescence of grain boundary located microcracks[20,21] (Fig. 7): a process that derives from the localized residual tensile stresses at grain boundaries (which develop due to thermal contraction anisotropy[22]). Fatigue mechanisms pertinent to the enhanced growth or coalescence of <u>microcracks</u> are thus of greatest relevance to many coarse grained ceramics. The appropriate distinction between the macrocrack

and microcrack regimes is emphasized in the following analyses of fatigue mechanisms.

The fatigue mechanisms that have been invoked in all prior analyses include considerations of localized plasticity and the concomittent stress reversal (and sometimes reversed plasticity) that occurs upon unloading. An example of such a phenomenon in ceramics is indentation fracture[11,23]. However, generalized crack tip plasticity does not occur in most ceramics[5]. An analogous fatigue treatment for ceramics must, therefore, invoke alternate modes of plasticity; such as indentation at crack surface asperities or the deformation of metallic second phases. Alternately, a completely different source of fatigue must be sought.

3.1 Tension/Compression Fatigue

a) Macrocrack Fatigue Mechanisms: Consideration will firstly be afforded to possible effects of plasticity. Plasticity in single phase polycrystalline ceramics could develop at crack surface asperities, whenever a macrocrack is subjected to normal compression (Fig. 8). Contacting asperities form on crack surfaces because of the relative displacements that occur when a crack relieves the localized residual stresses created by thermal contraction anisotropy. Very large stresses develop at the asperity contacts under an applied compression: stresses that could exceed the hardness, H, of the material. The resultant plasticity may lead to the formation of lateral cracks on unloading. These cracks could be of sufficient length to constitute an extension of the crack front (Fig. 8) during the compressive half cycle. To examine the viability of the mechanism, consider the relation for the lateral crack length, c[11];

$$(c/a)^2 = \frac{(HE^5)^{1/6}\sqrt{a}}{K_c} \qquad (12)$$

where E is Young's modulus, a is the contact radius and K_c is the fracture toughness. Introducing an asperity contact radius of ~2μm and using the properties of alumina (K_c ~4MPa $\sqrt{m}$, H ~ 20 GPa, E ~ 420 GPa), the lateral crack length would be ~6 μm. Lateral cracking of this extent would constitute a significant crack extension if an asperity of this magnitude could develop at a distance <4 μm from the crack tip (Fig. 8). The process thus appears plausible. However, evidence of this process should be clearly apparent on the fracture surface as plastic indentation and radial cracking at asperity locations. Such evidence should be sought before invoking this mode of fatigue crack growth.

An alternate role of the crack surface asperities might be connected with their influence on crack surface closure during unloading and subsequent compressive loading (Fig. 9). The asperities can cause the crack opening displacements to be maintained at relatively large levels throughout a tension, compression cycle. If the crack opening at peak tensile loading is maintained by the asperity closest to the crack tip, the crack opening 2h at that asperity is related to the peak stress intensity factor in the tensile half cycle $\hat{K}$ by[24];

$$\hat{K} = \frac{\sqrt{2\pi}\,\mu h}{(1-2\nu)\sqrt{r}} \tag{13}$$

where μ is the shear modulus, ν is Poisson's ratio and r is the distance of the asperity from the crack tip (Fig. 9). The magnitude of the stress intensity factor must change as the load is removed, and continue to change as the applied load becomes compressive. If the asperities do not deform plastically, the minimum closure that can occur during the compressive cycle is a uniform closure 2h for all locations beyond the first asperity (Fig. 9).

The stress intensity factor K^c for a crack separated by a zone of uniform thickness 2h is[25];

$$K^c = \left[\frac{2}{\pi(1-\nu)}\right] \frac{\sqrt{2\pi\mu h}}{\sqrt{r}} \tag{14}$$

This K value represents an upper bound for the stress intenstiy factor that can be maintained in the compressive half cycle. Comparison of Eqn. (13) and (14) shows that

$$\hat{K}/K^c = \pi(1-\nu)/2(1-2\nu). \tag{15}$$

The stress intensity factor in the compressive half cycle thus decreases to a level $\gtrsim 0.5\hat{K}$. Hence, the asperities cannot be the source of a fatigue mechanism. However, it should be noted that the maintenance of a relatively large K throughout the cycle would lead to violations of the quasi-static, cyclic comparator relations (such as Eqn. 8). Experimental results interpreted on the basis of these relations could thus provide misleading information about the existence of a fatigue effect. Examination of frequency effects[14] would be a more pertinent method for identifying fatigue.

b) Microcrack Fatigue Mechanisms: Fully-brittle ceramics may be amenable to fatigue under special circumstances. In particular, coarse-grained anisotropic ceramics that fracture by microcrack formation and coalescence might be prone to micro-structurally-related fatigue effects. An example is provided below. Consider the microstructure depicted in Fig. 10, in which microcracking of non-planar grain boundaries is an essential constituent in the fracture sequence illustrated in Fig. 7. Potential fatigue effects occur when such boundaries are inclined to the applied stress.

Examine an inclined boundary containing a microcrack, which has propagated to a length 2a by slow crack growth in the tensile half cycle; the path of subsequent propagation then deviates toward the direction of the applied stress (Fig. 10). The subsequent extension of the crack is governed by the stress intensity factor pertinent to a kinked crack[26] (Fig. 11). This stress intensity factor is given by the relations[26],

$$K_I = \kappa_{11}(\alpha)K_I^m + \kappa_{12}(\alpha)K_{II}^m$$
$$K_{II} = \kappa_{21}(\alpha)K_I^m + \kappa_{22}(\alpha)K_{II}^m \qquad (16)$$

where K_I^m and K_{II}^m are the stress intensity factors for the main crack (modes I and II respectively) and the κ terms are coefficients that depend on the kink angle α, as plotted in Fig. 11. Propagation of the crack is assumed to be dictated by the coplanar strain energy release rate criterion[27];

$$K^2 \approx K_I^2 + K_{II}^2 \qquad (17)$$

The stress intensity factors K^m have a component due to the residual stress (that derives from thermal contraction anisotropy) as well as that due to the applied stress[22]. Hence, in the tensile half cycle, the resultant stress intensity factor obtained from Eqns. (16) and (17) is

$$\frac{K^2}{\pi a} = \kappa_{11}(\alpha)\left[(\sigma^R + \sigma_\infty^T\cos^2\theta) + \kappa_{12}(\alpha)\,(\pm\tau^R + \sigma_\infty \sin\theta\cos\theta)\right]^2$$
$$+ \kappa_{21}(\alpha)\left[(\sigma^R + \sigma_\infty^T\cos^2\theta) + \kappa_{22}(\alpha)\,(\pm\tau^R + \sigma_\infty^T \sin\theta\cos\theta)\right]^2 \qquad (18)$$

where σ^R and τ^R are the residual normal and shear stresses respectively (averaged over the crack plane) and θ is the inclination of the main crack plane normal to the applied tensile stress σ_∞^T. The corresponding stress intensity factor for the compressive half cycle is;

$$\frac{K^2}{\pi a} = \left[\kappa_{11}(\alpha)\ (\sigma^R - \sigma_\infty^c \cos^2\theta) + \kappa_{12}(\alpha)\ (\pm\tau^R - \sigma_\infty^c \sin\theta\cos\theta)\right]^2 + \left[\kappa_{21}(\alpha)\ (\sigma^R - \sigma_\infty^c \cos^2\theta) + \kappa_{22}(\alpha)\ (\pm\tau^R - \sigma_\infty^c \sin\theta\cos\theta)\right]^2 \quad (19)$$

where σ_∞^c is the applied compressive stress. This relation pertains whenever $\sigma^R > \sigma_\infty^c \cos^2\theta$, i.e., when a finite crack opening is maintained so that crack surface friction[28] does not negate the stress intensification. The residual stress can be very large in many ceramics[22], this condition would thus be satisfied in a variety of practical situations. Examination of Eqns. (18) and (19) indicates that, because $\kappa_{12}(\alpha)$ is negative (Fig. 11), K in the compressive cycle can exceed that in the tensile cycle. The fundamental requirement for the existence of fatigue is thus satisfied. Namely, obstacles to the continued motion of cracks subject to applied tension are more readily circumvented under an applied compression; thereby permitting the total growth under combined tension/compression to exceed that expected under simple tension. The magnitude of the fatigue, of course, depends upon the specific values of σ^R, θ, α and σ_∞; in fact, fatigue will only manifest itself when these controlling variables lie within certain ranges. A readily comprehended fatigue condition is illustrated in Fig. 10b. For this condition the applied tensile stress augments the residual shear stress, such that both stresses tend to induce crack closure in the region of the kink.

For example, if $\theta = \alpha = 45°$, the mode I component of K at the kink becomes;

$$K_I^T = 0.8\sigma^R - \tau^R - 0.1\sigma_\infty^T \tag{20}$$

and hence, for $\tau^R + 0.1\,\sigma_\infty^T > 0.8\sigma^R$, K_I is negative and crack closure is experienced. Thereupon, crack surface friction prevents the development of a mode II stress intensification and the crack cannot propagate. However, the equivalent stress intensity factor in compression is;

$$K_I^C = 0.8\sigma^R - \tau^R + 0.1\sigma_\infty^C \tag{21}$$

Hence, conditions under which K_I is positive (which also permit a finite crack opening to be maintained on the main crack ($\sigma_\infty^C < 2\,\sigma_R$)) can be found: thereby, allowing crack propagation to proceed by a combination of K_I^C and K_{II}^C. A condition that would produce crack propagation in compression but not in tension is: $\tau^R = 0.8\sigma^R$, $\sigma_\infty^{T,C} = \sigma^R$. For this condition the stress intensity factor under compression is

$$K^C \sim 0.37\sigma_\infty^C \sqrt{\pi a} \tag{22}$$

while the stress intensity factor on the main crack during the tensile crack just prior to kinking would be

$$K^T = 0.71\sigma_\infty^T \sqrt{\pi a} \tag{23}$$

and of course, just after kinking, the effective K^T reduces to zero.

The microstructurally-related fatigue mode described above could account for the observations of Guiu[18]; whose studies were conducted on a material (coarse grained alumina) that typically fails by a microcrack formation and coalescence process[20].

3.2 Fatigue In Ceramics/Metal Systems

The presence of a metallic constituent within a ceramic, especially as a continuous phase, introduces the potential for fatigue, according to the mechanisms conventionally invoked for fatigue in metals. It is appropriate, however, to consider variations that might pertain in ceramic/metal systems. Specific attention will be devoted to the WC/Co system because quantitative results are available for this system[14]. However, the mechanisms proposed could be generally encountered in ceramic/metal systems.

Whenever a continuous metallic phase exists, a crack must encounter the metallic phase. Then, because of the substantially superior toughness of the metal, ligaments of metal are expected to remain behind the primary crack front[29] (Fig. 12). Ductile failure of the ligaments produces the ductile dimple features observed on the fracture surface in the metal phase[30], as determined by the careful fracture surface matching studies of Luychx[31]. These ligaments supply crack closure forces, which can be considered as a primary source of toughness in this class of materials. Treating the ligaments as a simple Dugdale zone, the toughness in the presence of ligaments can be shown to depend on the flow strength σ_y of the metal phase, and the dispersion of the phase, through the relation[29];

$$K_c = K_o + \frac{\sigma_y}{(1+d/D)^2}\sqrt{\frac{\pi L}{2}} \qquad (24)$$

Where K_o is the intrinsic toughness of the ceramic constituent, or of the ceramic/metal interface (whichever is preferred site for crack extension), d is the separation between ligaments, D is the ligament diameter and L is the length of the ligament zone. Inserting values of these parameters pertinent to WC/12% Co[30,31,32] ($K_c \sim 16\text{MPa}\sqrt{\text{m}}$, $K_o \sim 4\text{MPa}\sqrt{\text{m}}$, $\sigma_y \sim 3\text{GPa}$,

d/D ~ 0.13) yields a ligament zone size of 20 μm. This magnitude is reasonably consistent with observations of the distance from the crack tip at which the metal constituent remains intact[23].

The ligaments at the perimeter of the zone will be subject to extensive plastic strain, and can be expected to exhibit necking (Fig. 12). Hence, when the applied load is reduced and the crack surface separation diminishes, plastic buckling and failure is likely to occur in the peripheral ligaments. The effective ligament zone width and hence, the total closure force, is thus reduced by an amount ΔL. Upon subsequent application of stress the stress intensity factor pertinent to crack extension becomes;

$$K = K_\infty - \frac{\sigma_y}{(1 + d/D)^2} \sqrt{\frac{\pi(L - \Delta L)}{2}} \tag{25}$$

where K_∞ is the applied stress intensity factor ($K_\infty = \sigma_\infty^T \sqrt{\pi a}$). IF K exceeds the intrinsic toughness K_o of the matrix the crack will extend during the tensile cycle and fatigue will be observed. Superimposing this condition, Eqns. (24) and (25) indicate that fatigue will be observed whenever $K_\infty > K^*$, where;

$$K^* = K_c - (K_c - K_o)(\Delta L/2L) \tag{26}$$

The resulting crack growth Δa that occurs when the peak stress intensity factor K exceeds K* is,

$$\frac{\Delta a}{L} = \frac{\Delta L}{L} + \left(\frac{\hat{K} - K_o}{K_c - K_o}\right)^2 - 1 \tag{27}$$

The ligament failure zone ΔL evidently depends on K_{min} and the detailed physical

properties of the metallic phase. Insufficient details of the behavior of the metal are presently available for further analysis. However, it is directly evident from Eqn. (27) that the crack growth per cycle $\Delta a/\Delta N$ will depend on cycle parameters in additional to the stress intensity factor range $\Delta K(=\hat{K} - K_{min})$, in accord with the existing observations[14].

CONCLUSIONS

It has been demonstrated that there are few unequivocal observations of fatigue in ceramics. Many effects interpreted as fatigue are, upon more detailed examination, various manifestations of environmentally induced slow crack growth. One of the more significant conclusions is thus the need for additional (definitive) experiments which clearly define the conditions that encourage fatigue.

Fatigue mechanisms have been suggested pertinent to two situations where experimental evidence strongly favours the existence of fatigue: viz., under tension/compression cycling and in ceramic/metal systems. The fatigue degradation in both cases depended upon microstructural details and no simple degradation relations, analagous to $da/dN \alpha F(\Delta K)$, emerged. Experimental observations are again needed to study the role of the parameters suggested by the models on the extent of the fatigue process

ACKNOWLEDGMENT

This work was supported by the Division of Materials Sciences, Office of Basic Energy, U.S. Department of Energy under contract No. W-7405-Eng-48.

REFERENCES

1. R.E. Mould and R.D. Southwick, Jnl. Amer. Ceram. Soc., 42 (1959) 589.
2. T.C. Baker and F.W. Preston, Jnl. Appl. Phys., 17 (1946) 189.
3. J.E. Burke, R.H. Doremus, W.B. Hillig and A.M. Tuskalo, 'Ceramics in Severe Environments (Ed., V.W. Kriegel and H. Palmour) Plenum, N.Y. (1971).
4. R.N. Katz, work performed at AMMRC, private communication.
5. S.M. Wiederhorn, B.J. Hockey and D.W. Roberts, Phil. Mag., 28 (1973) 783.
6. A.L. Pranatis, Jnl. Amer. Ceram. Soc., 52 (1969) 340.
7. G.G. Garrett, H.M. Jennings and R.B. Tait, Jnl. Mater. Sci., 14 (1979) 296.
8. J. McLaren and R.W. Davidge, Proc. Brit. Ceram. Soc., 25 (1975) 112.
9. A.G. Evans, S.M. Wiederhorn, M. Linzer and E.R. Fuller, Bull Amer. Ceram. Soc., 54 (1975) 576.
10. R.W. Rice, private communication.
11. B.R. Lawn, A.G. Evans and D.B. Marshall, Jnl. Amer. Ceram. Soc., in press.
12. G. Sines, Jnl. Amer. Ceram. Soc., 59 (1976) 370.
13. A.G. Evans and E.R. Fuller, Met Trans, 5 (1974) 27.
14. A.G. Evans and M. Linzes, Int'l. Jnl. Frac., 12 (1976) 217.
15. A.G. Evans, L.R. Russell and D.W. Richerson, Met. Trans., 6A (1975) 707.
16. D.A. Krohn and D.P.H. Hasselman, Jnl. Amer. Ceram. Soc., 55 (1972) 208.
17. C.P. Chen and W.J. Knapp, Fracture Mechanics of Ceramics (Ed. R.C. Bradt, D.P.H. Hasselman and F.F. Lange) Plenum, N.Y. (1947) vol. 2, p. 691.
18. F. Guiu, Jnl. Mater. Sci., 13 (1978) 1357.
19. R. Kossowsky, D.G. Miller and E.S. Diaz, Jnl. Mater. Sci., 10 (1975) 983.
20. A.G. Evans, L.R. Russell and M. Linzer, Mat. Sci. Eng., 15 (1974) 253.
21. F.A. McClintock and H.J. Mayson, ASME Applied Mechanics Conference (June 1976).
22. A.G. Evans, Acta Met., 26 (1978) 1845.
23. B.R. Lawn and T.R. Wilshaw, Jnl. Mater. Sci., 10 (1975) 1049.
24. B.R. Lawn and T.R. Wilshaw, Fracture of Brittle Solids (Cambridge Univ. Press), Cambridge 1975.
25. G.I. Barenblatt, Adv. Appl. Mech. Academic Press, N.Y., 7 (1962).

26. B.A. Bilby, G.E. Cardew and I.C. Howard, Fracture 1977, (Ed. D.M.R. Taplin) Univ. Waterloo Press, vol. 3 (1977) p. 197.

27. J.J. Petrovic and M.G. Mendiratta, Jnl. Amer. Ceram. Soc., 60 (1977) 403.

28. F.A. McClintock and J.B. Walsh, Proc. 4th U.S. Nat'l. Congr. Appl. Mech. (U.C. Berkeley), 1962, p. 1015.

29. A.G. Evans, A.H. Heuer and D. Porter, Fracture 1977 (Ed. D.M.R. Taplin), Univ. Waterloo Press, vol. 1 (1977) p. 529.

30. J.L. Chermant, A. Deschanvres and A. Iost, Fracture Mechanics of Ceramics (Ed. R.C. Bradt, D.P.H. Hasselman and F.F. Lange) Plenum, N.Y., vol. 1 (1974) p. 347.

31. S.B. Luychx, Fracture 1977 (Ed. D.M.R. Taplin), Univ. Waterloo Press, vol. 2 (1977) p. 223.

32. L. Lindau, ibid, p. 215.

33. J.L. Chermant and F. Osterstock, ibid, p. 229.

FIGURE CAPTIONS

Fig. 1: The parameter g that relates the cyclic to the quasi-static crack velocity, plotted as a function of the cycle amplitude and the exponent n.

Fig. 2: A comparison of cyclic and quasi-static crack velocities with the predictions derived using Fig. 1 (a) porcelain, (b) glass.

Fig. 3: A comparison of cyclic time-to-failure data with the prediction derived from the static data and from Fig. 1 (after Krohn and Hasselman).

Fig. 4: A comparison of static and cyclic failure time data for polycrystalline alumina (after Chen and Knapp).

Fig. 5: A plot of the failure time for alumina samples subject to static stress and tension/compression cyclic stress (after Guiu).

Fig. 6: Cyclic crack propagation data obtained on WC/12% Co at two different average stress intensity factors.

Fig. 7: The sequence involved in failure by microcrack formation and coalescence.

Fig. 8: The formation of lateral cracks at crack surface asperities.

Fig. 9: The limitation on crack closure provided by the crack surface asperities.

Fig. 10: A microcrack extension process that can lead to a fatigue effect.

Fig. 11: The stress intensity factor parameters pertinent to a kinked crack (after Bilby et. al.).

Fig. 12: Plastic ligaments that provide closure tractions in certain ceramic/metal systems.

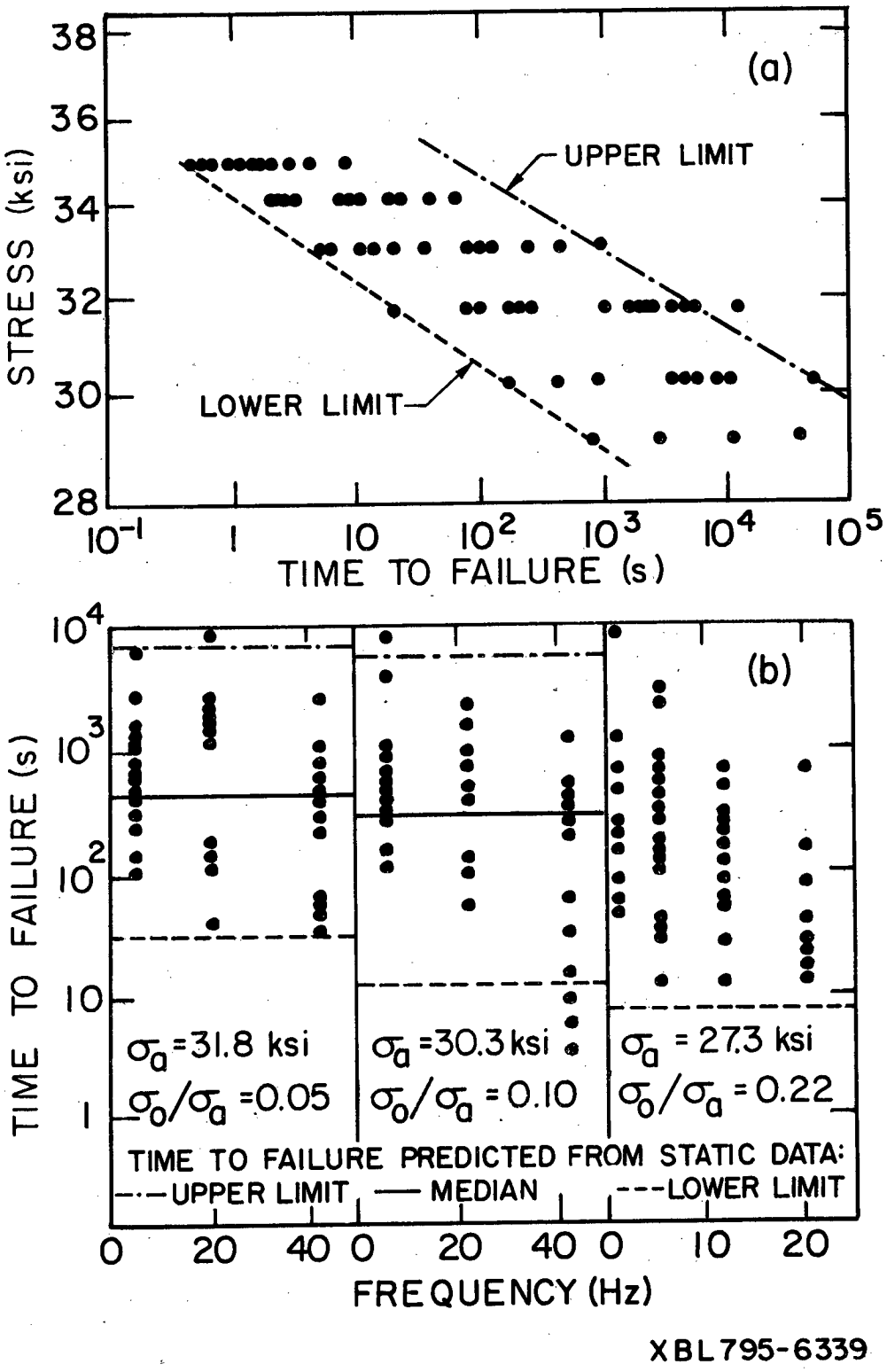
(a)
STRESS (ksi)
38
36
34
32
30
28
UPPER LIMIT
LOWER LIMIT
10^{-1}
1
10
10^2
10^3
10^4
10^5
TIME TO FAILURE (s)
(b)
TIME TO FAILURE (s)
10^4
10^3
10^2
10
1
σ_a =31.8 ksi
σ_0/σ_a =0.05
σ_a =30.3 ksi
σ_0/σ_a = 0.10
σ_a = 27.3 ksi
σ_0/σ_a = 0.22
TIME TO FAILURE PREDICTED FROM STATIC DATA:
UPPER LIMIT
MEDIAN
LOWER LIMIT
0
20
40
0
20
40
0
10
20
FREQUENCY (Hz)
XBL795-6339

Figure 1

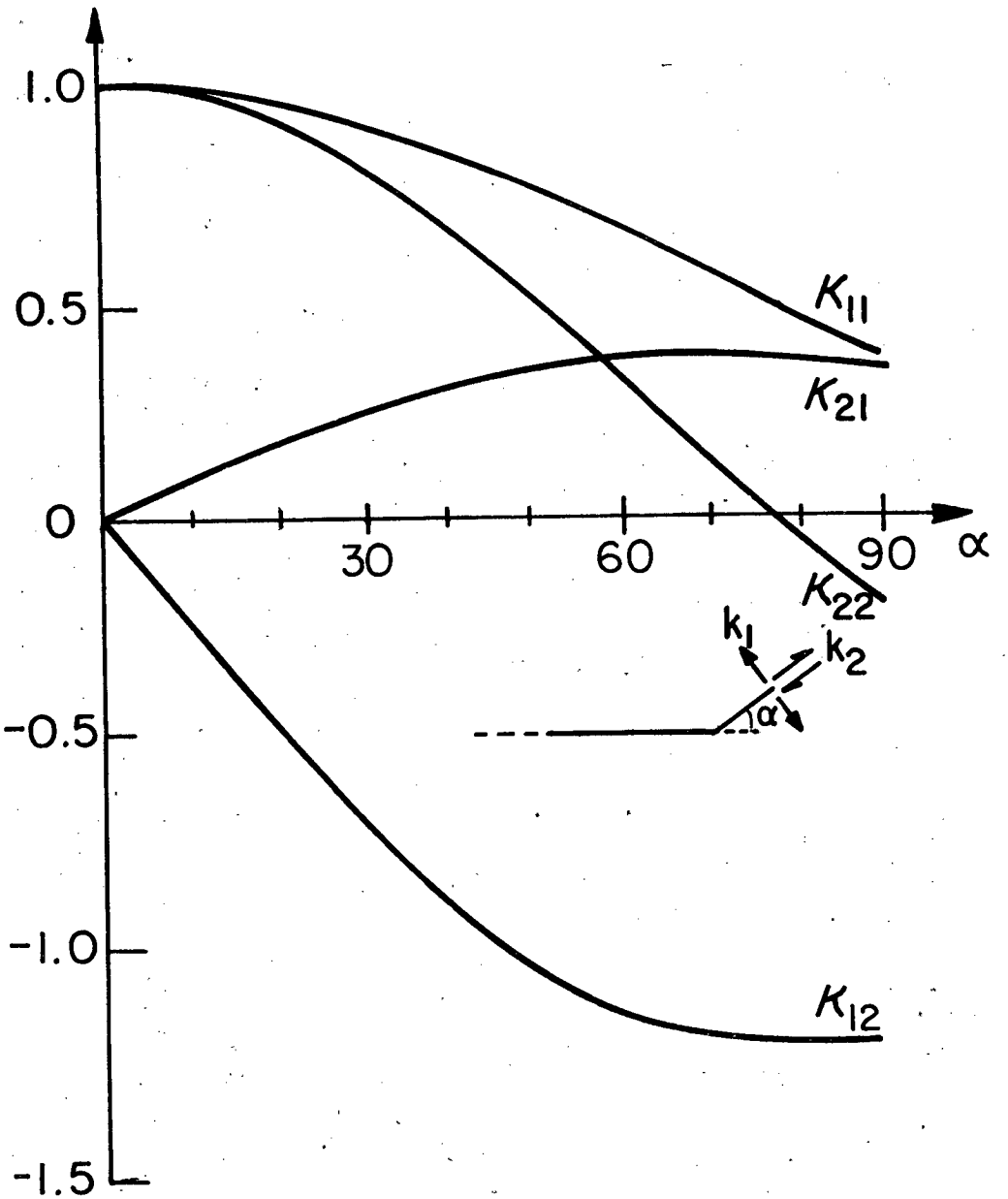

XBL 795-6340

Figure 2

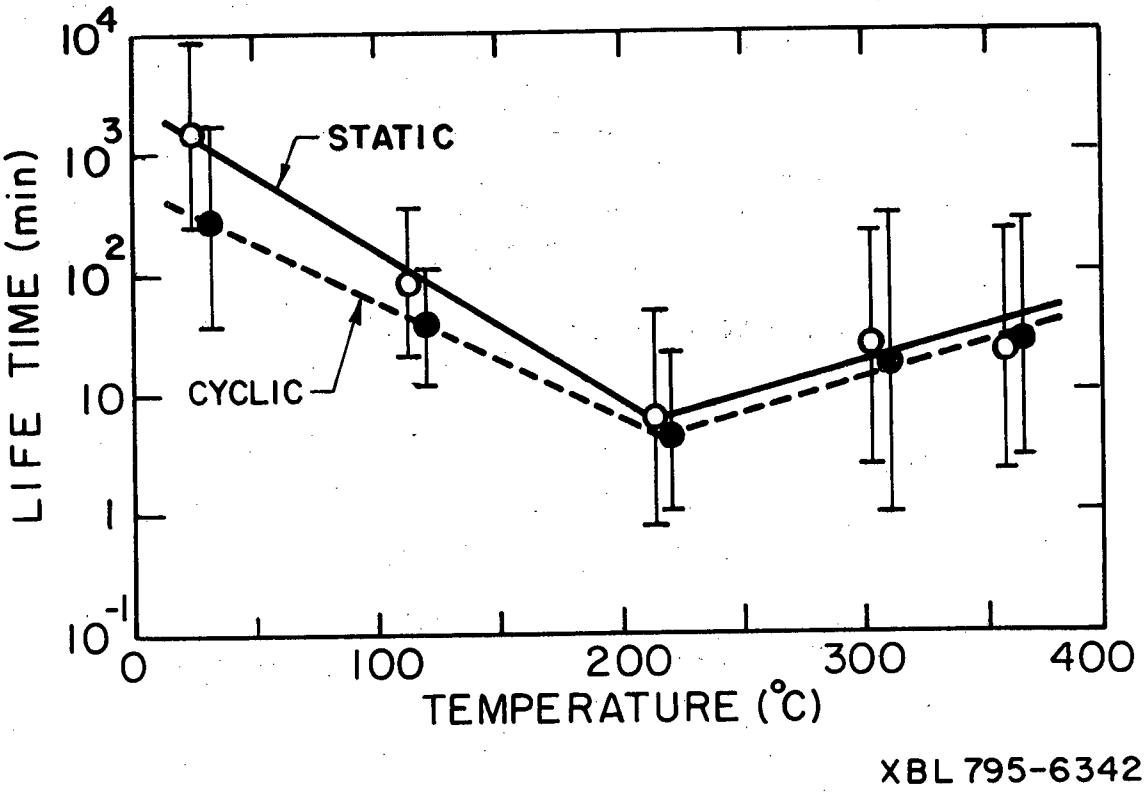
LIFE TIME (min)
10^4
10^3
10^2
10
1
10^{-1}
STATIC
CYCLIC
0
100
200
300
400
TEMPERATURE (°C)
XBL 795-6342

Figure 3

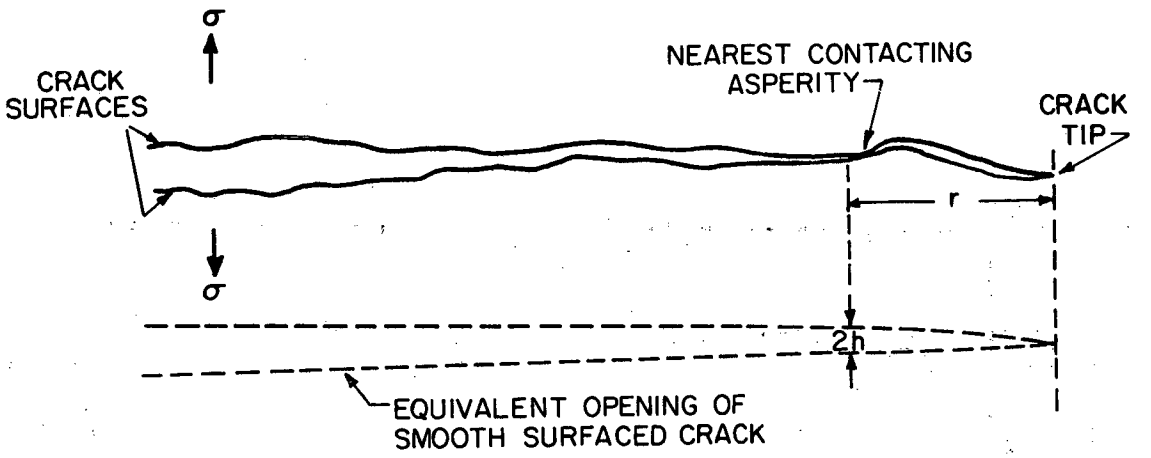

(a) CRACK AT PEAK APPLIED TENSILE STRESS

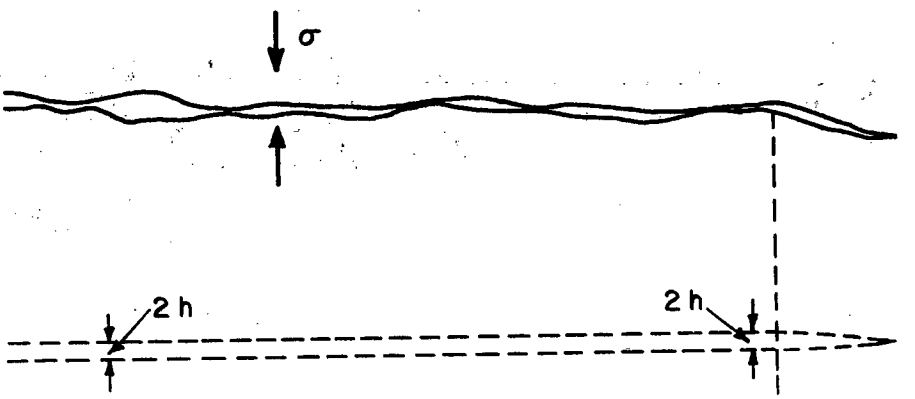

(b) COMPLETE ASPERITY CONTACT UNDER APPLIED COMPRESSION

XBL 795-6331

Figure 4

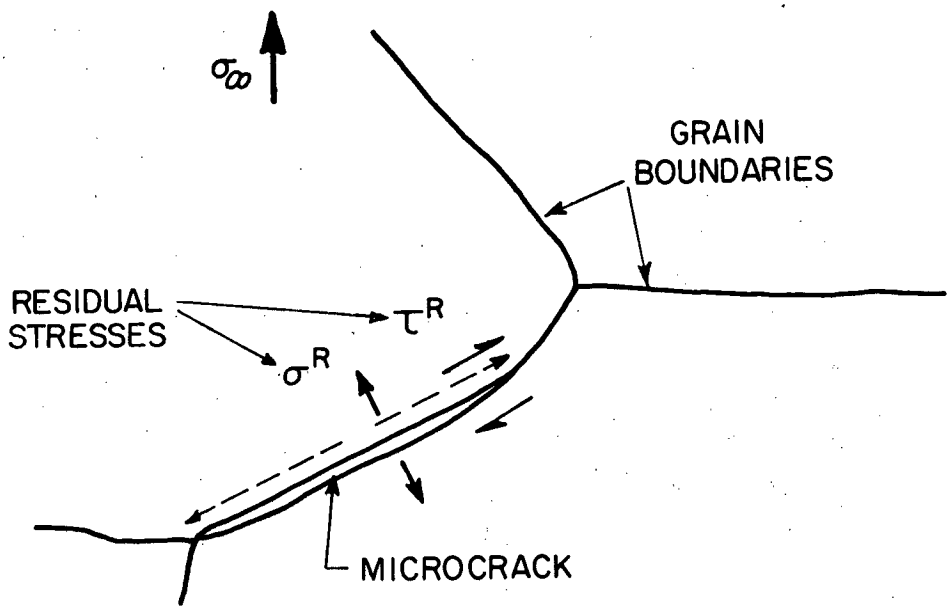

(a) FATIGUE PRONE MICROSTRUCTURE

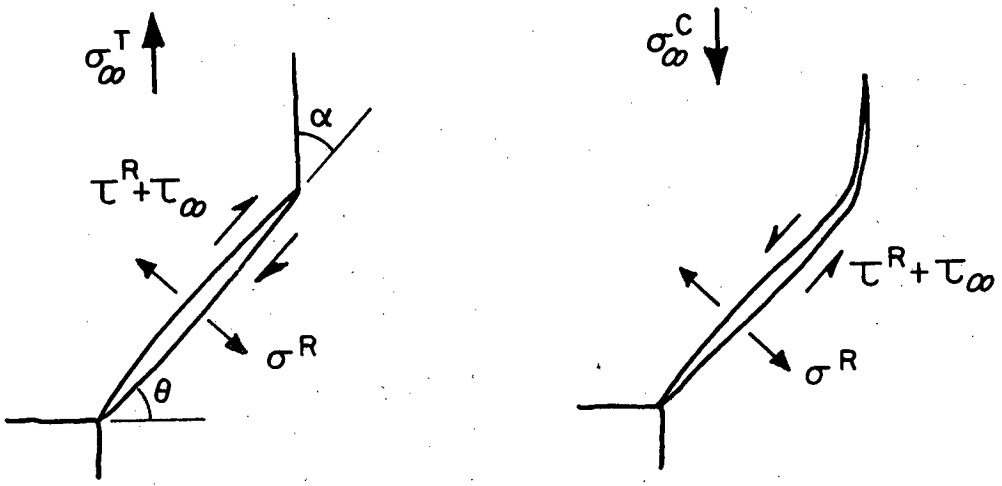

(b) SCHEMATIC OF FATIGUE CONDITION

XBL795-6332

Figure 5

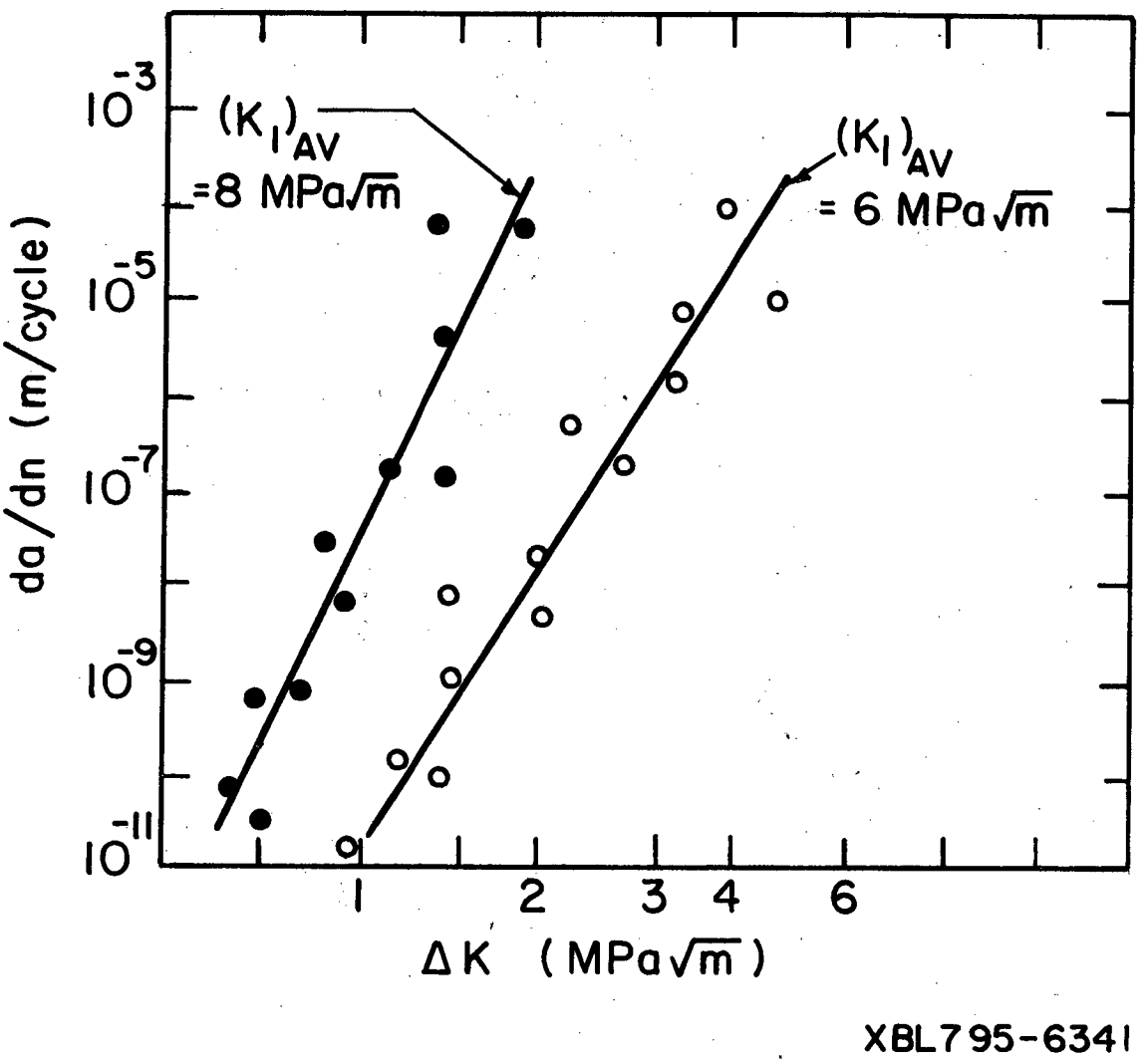
10^{-3}
10^{-5}
10^{-7}
10^{-9}
10^{-11}
da/dn (m/cycle)
$(K_I)_{AV}$
=8 MPa$\sqrt{m}$
$(K_I)_{AV}$
= 6 MPa$\sqrt{m}$
1
2
3
4
6
ΔK (MPa$\sqrt{m}$)
XBL795-6341

Figure 6

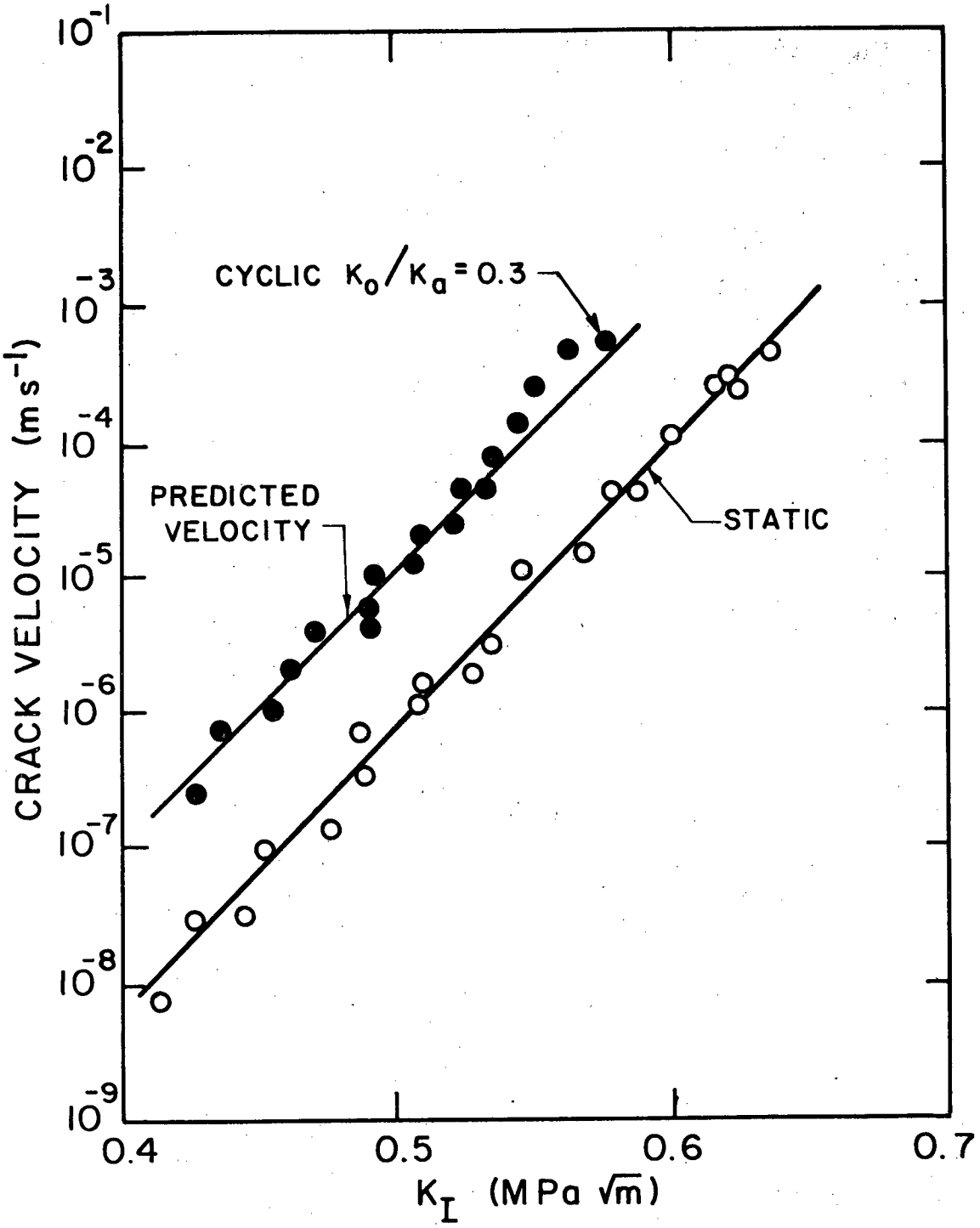
CYCLIC $K_o/K_a = 0.3$
PREDICTED VELOCITY
STATIC
CRACK VELOCITY (m s^{-1})
10^{-1}
10^{-2}
10^{-3}
10^{-4}
10^{-5}
10^{-6}
10^{-7}
10^{-8}
10^{-9}
0.4
0.5
0.6
0.7
K_I (MPa $\sqrt{m}$)
XBL 795-6338

Figure 7

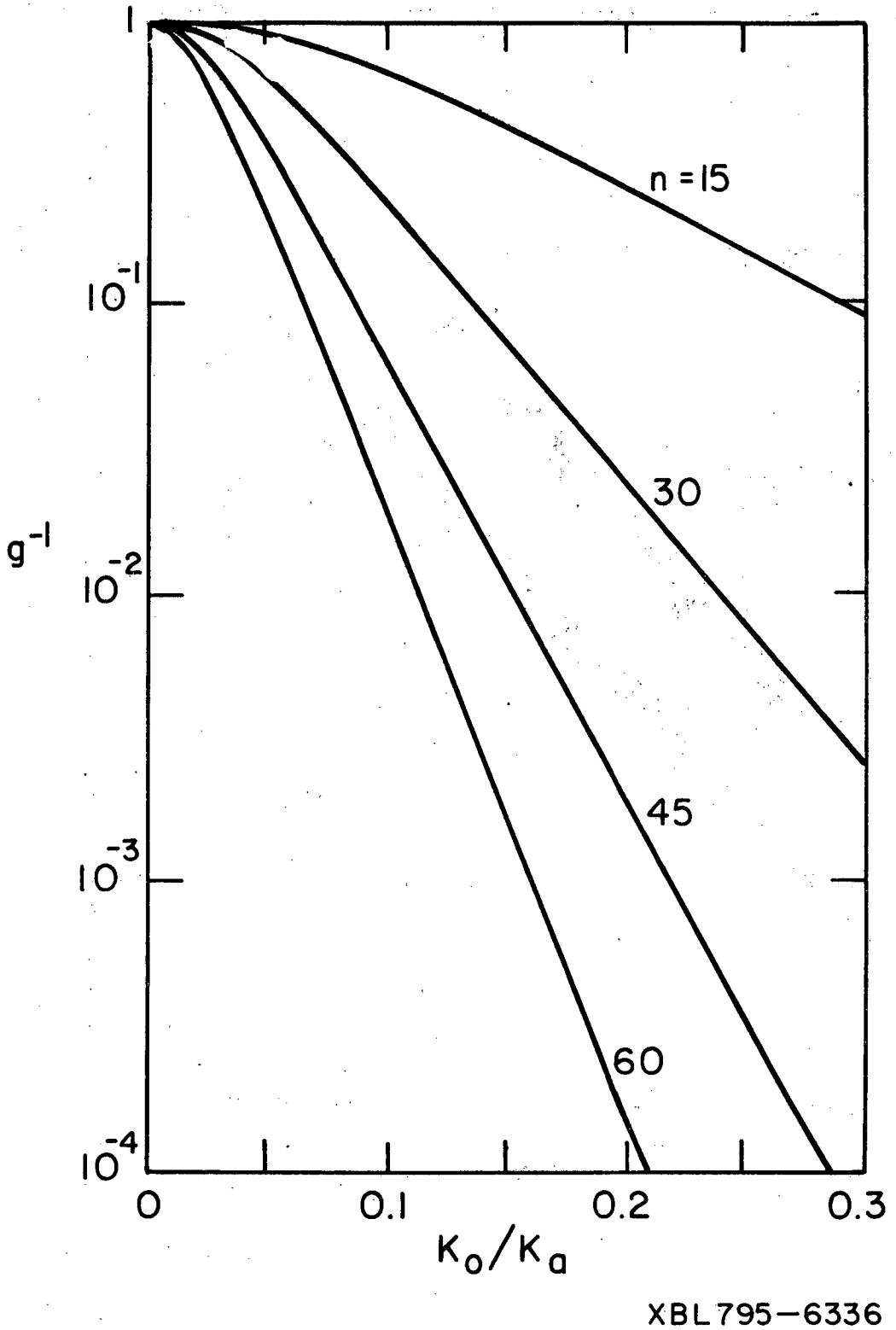

Figure 8

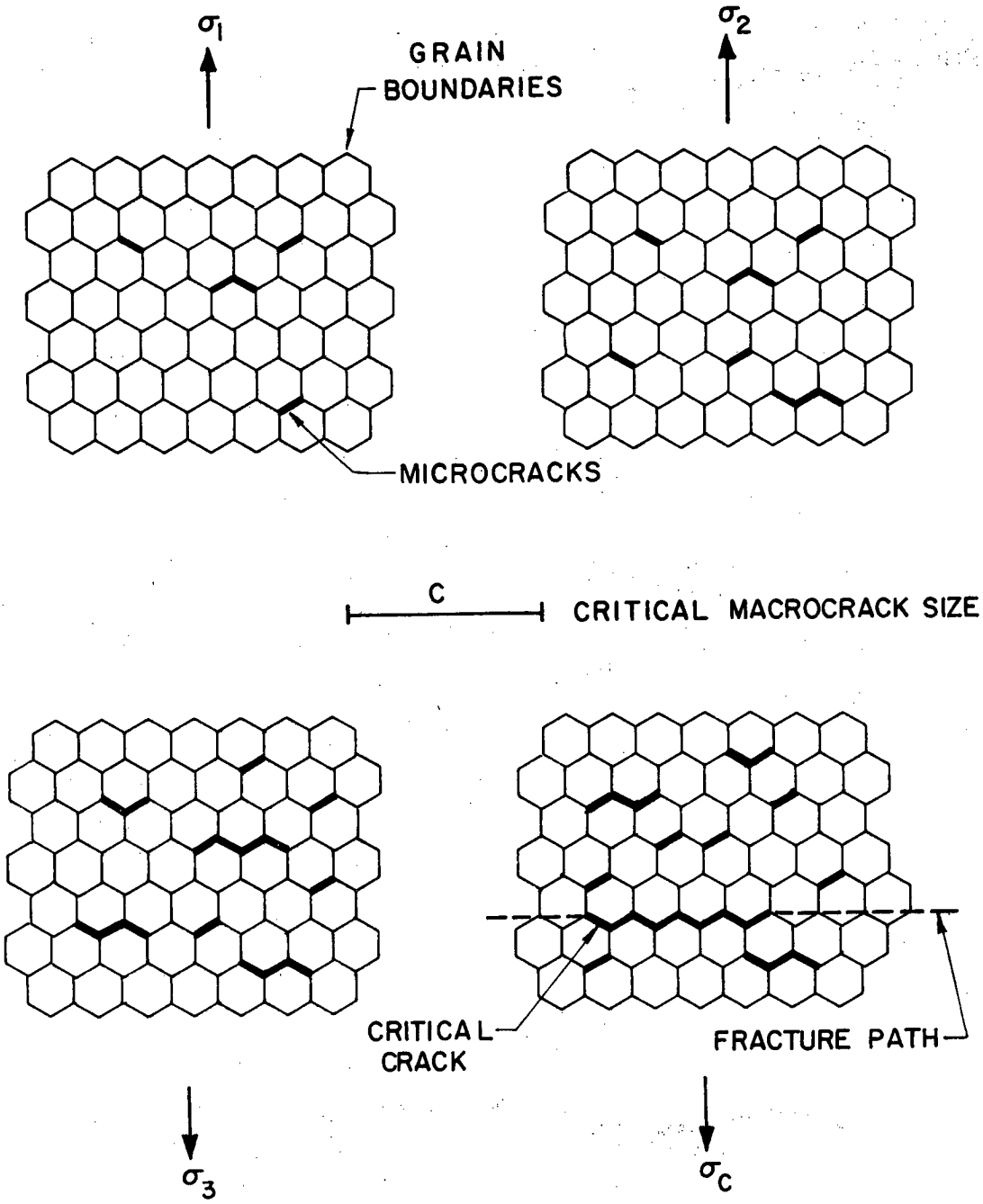
σ1
GRAIN
BOUNDARIES
σ2
MICROCRACKS
C
CRITICAL MACROCRACK SIZE
CRITICAL
CRACK
FRACTURE PATH
σ3
σC
XBL793-5995A

Figure 9

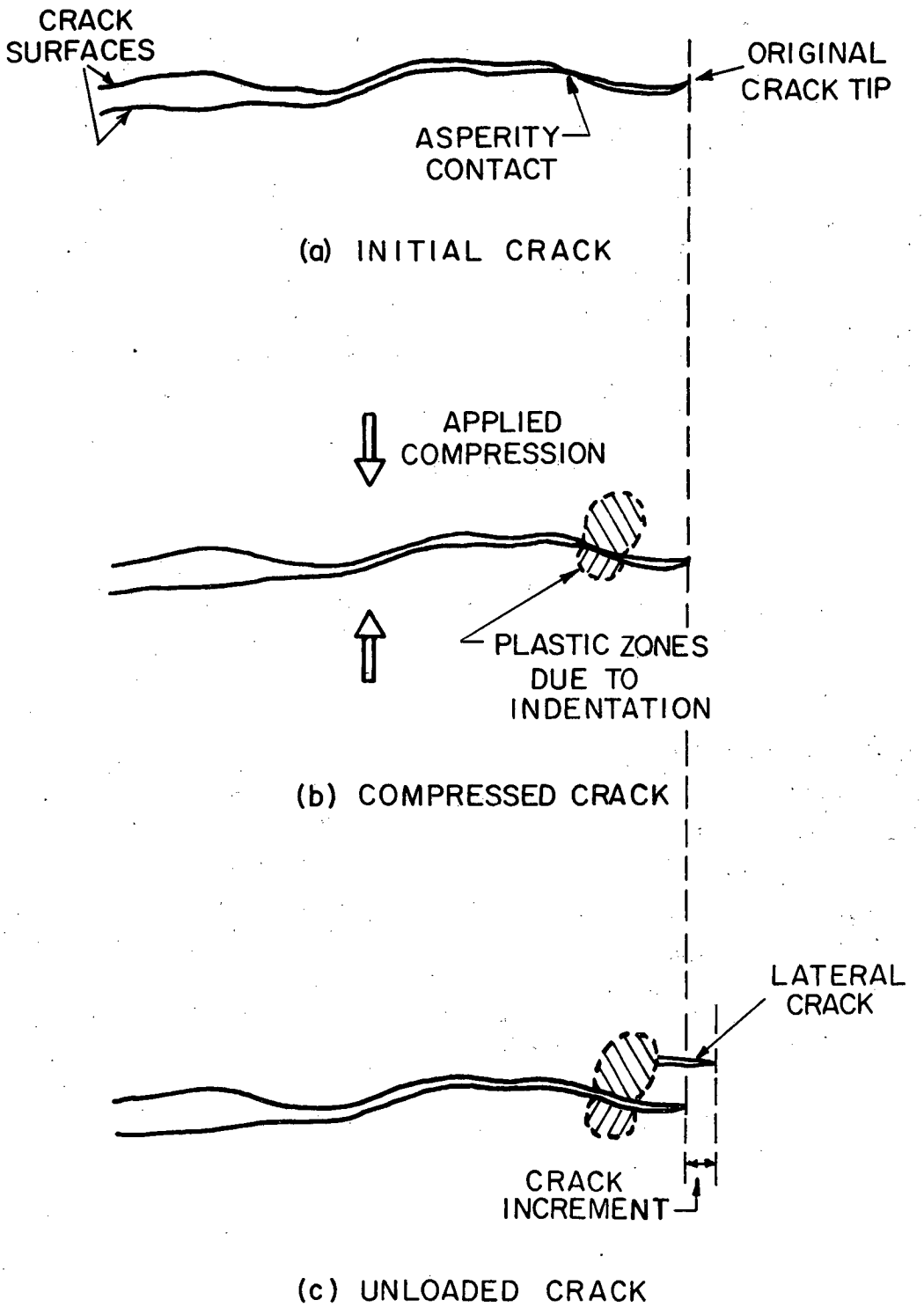
CRACK SURFACES
ORIGINAL CRACK TIP
ASPERITY CONTACT
(a) INITIAL CRACK
APPLIED COMPRESSION
PLASTIC ZONES DUE TO INDENTATION
(b) COMPRESSED CRACK
LATERAL CRACK
CRACK INCREMENT
(c) UNLOADED CRACK
XBL795-6333

Figure 10

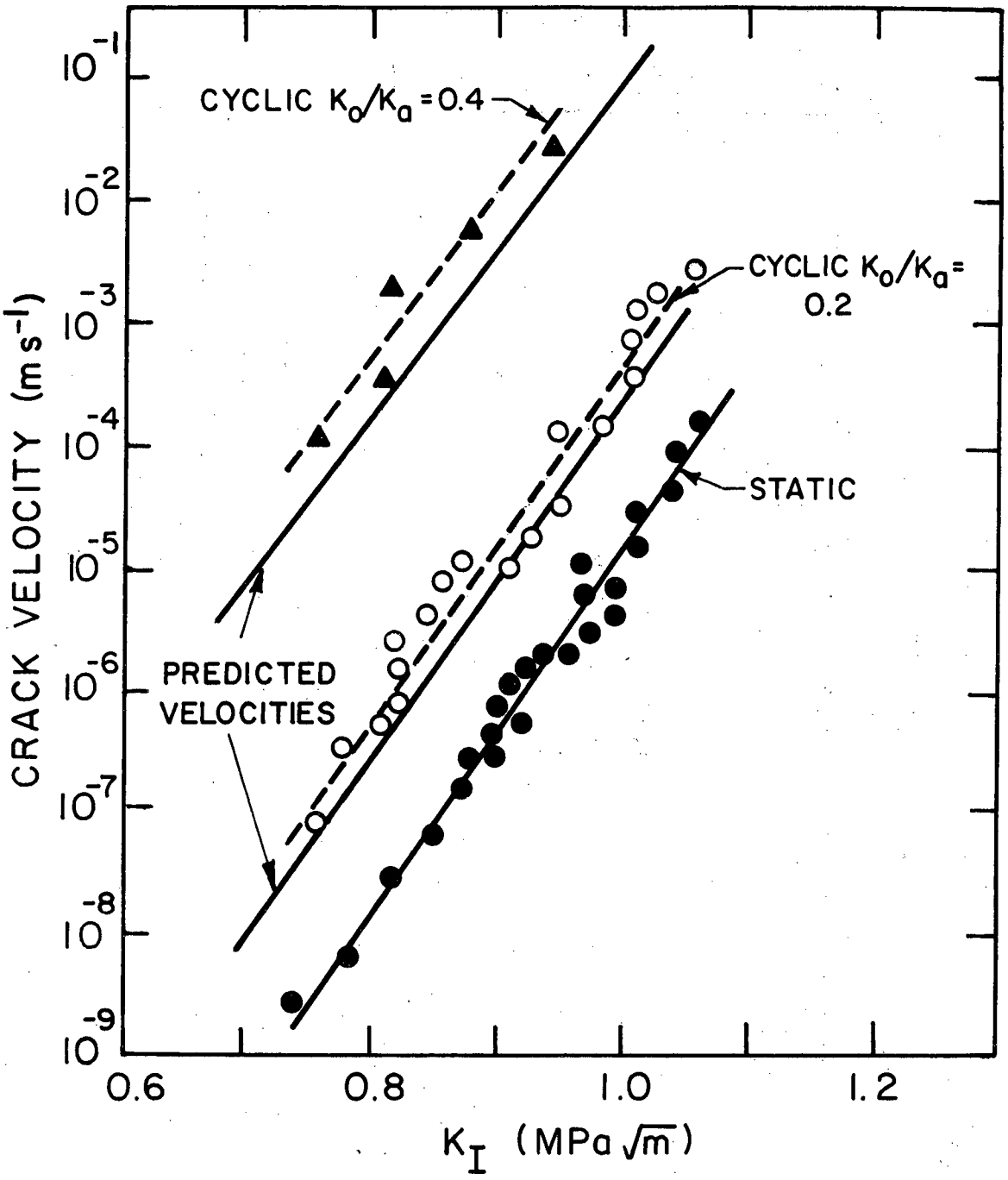
CYCLIC $K_o/K_a = 0.4$
CYCLIC $K_o/K_a =$ 0.2
STATIC
PREDICTED VELOCITIES
CRACK VELOCITY ($m\,s^{-1}$)
10^{-1}
10^{-2}
10^{-3}
10^{-4}
10^{-5}
10^{-6}
10^{-7}
10^{-8}
10^{-9}
0.6
0.8
1.0
1.2
K_I ($MPa\sqrt{m}$)
XBL795-6337

Figure 11

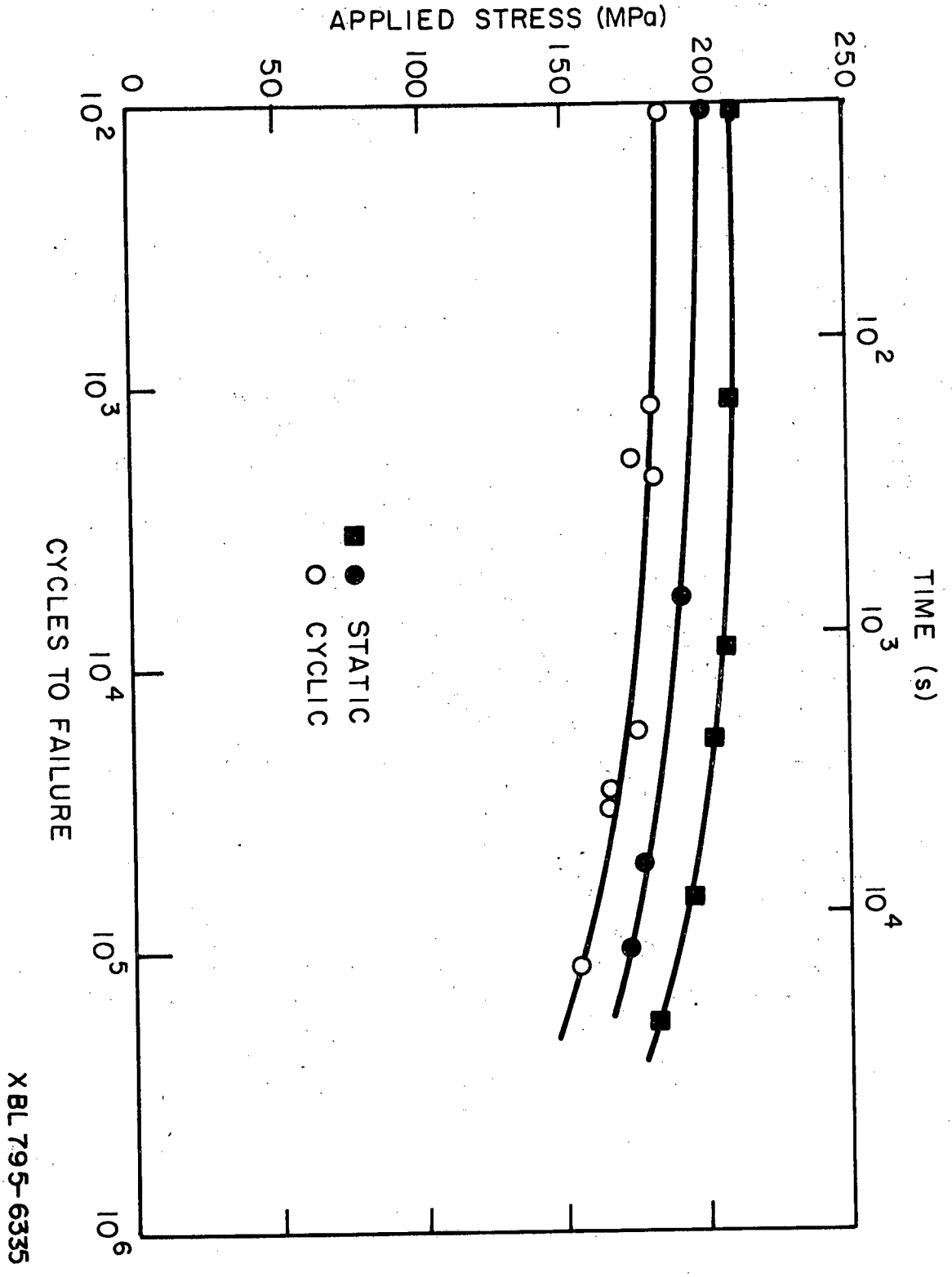
APPLIED STRESS (MPa)
0
50
100
150
200
250
10^2
10^3
10^4
10^5
10^6
CYCLES TO FAILURE
STATIC
CYCLIC
TIME (s)
10^2
10^3
10^4
XBL 795-6335

Figure 12

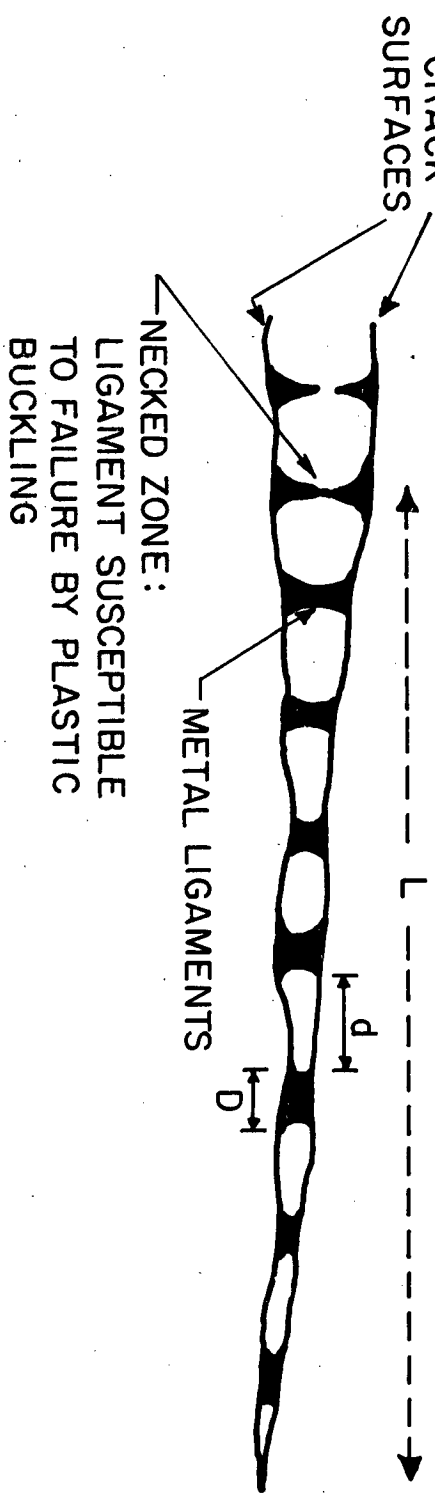
CRACK SURFACES
NECKED ZONE:
LIGAMENT SUSCEPTIBLE TO FAILURE BY PLASTIC BUCKLING
METAL LIGAMENTS
L
d
D
XBL 795-6334

Figure 13

TECHNICAL INFORMATION DEPARTMENT
LAWRENCE BERKELEY LABORATORY
UNIVERSITY OF CALIFORNIA
BERKELEY, CALIFORNIA 94720